

An organometallic route to zinc phosphonates and their intercalates

Philippe Gerbier,* Christian Guérin,* Bernard Henner and Jean-Rémi Unal

U.M.R. 5637 - Université Montpellier II, Place Eugène Bataillon – Case 007, 34095 Montpellier cedex 5, France. E-mail: gerbier@crit.univ-montp2.fr

Received 12th April 1999, Accepted 9th June 1999

An organometallic non-aqueous route to zinc phosphonates and to their intercalates has been studied. Various phosphonic acids react with dimethylzinc in THF media to afford the corresponding layered zinc phosphonates $Zn(O_3PR^1)$ ($R^1 = \text{Me, Ph, 2- and 3-thienyl, thiophen-3-ylmethyl}$) with evolution of methane. The presence of a primary *n*-alkylamine in the reaction mixture allows the one-pot formation of 2D-layered intercalated phases of general formula $Zn(O_3PR^1) \cdot R^2NH_2$ [$R^2 = \text{Bu}^n, \text{Pen}^n (=n\text{-pentyl})$] whereas a more bulky amine such as cyclohexylamine (Hex^cNH_2) lead to the formation of 1D polymeric chains of formula $Zn(O_3PPh) \cdot 2\text{Hex}^c\text{NH}_2$.

1 Introduction

There is currently high interest in designing hybrid organic-inorganic derivatives where the organic and inorganic components complement each other leading to solid-state structures and materials with composite or new properties.¹ Examples of interest are layered metal organophosphonates which have received considerable attention because of their structural chemistry and potential applications.²

The usual synthetic route to such derivatives uses hydrothermal conditions based on the reaction of a phosphonic acid RPO_3H_2 with a metal salt.³ Consequently, it excludes the use of a wide variety of phosphonic acids either owing to their restricted solubility or to their water and (or) thermal sensitivity.⁴ An alternative non-hydrolytic route to layered metal(IV) phosphonates based on thermal condensation between halide and alkoxide groups has recently been developed; however, the reactions are usually carried out at 100–150 °C in sealed tubes.⁵

To circumvent these difficulties, we anticipated that an organometallic route using organic-soluble precursors would be of interest. There have been successful attempts in the synthesis of group 13 and aluminium framework metallo-phosphonates through facile alkane elimination between a metal alkyl and a phosphonic acid.⁶ The analogous reaction of either $\text{HO(O)P(OBu}^1)_2$ or $\text{Bu}^1\text{PO}_3\text{H}_2$ with ZnEt_2 proved to yield an insoluble polymeric phosphate-based material $\{\text{ZnO}_2\text{P(OBu}^1)_2\}_n$ or a large cage-shaped zinconophosphonate $[\text{Zn}_2(\text{thf})_2(\text{EtZn})_6\text{Zn}_4(\mu^4\text{-O})(\text{Bu}^1\text{PO}_3)_8]$, respectively.⁷ The mild and non-aqueous conditions required in the latter reactions should provide a useful approach to layered organophosphonates with ordered organic and (or) organometallic functional side-groups. Moreover, besides structural variations depending on the phosphonic acids and the solvent, it should facilitate new entries into their intercalation chemistry.^{5,8} In this work, we focus exclusively on the production of zinc phosphonates and their intercalates.

2 Experimental

2.1 General

Keys for the understanding of compound notation: **a** indicates that the compound is related to the gel-like phosphonates, **b** indicates that the compound was prepared following literature methods and **c** indicates that the compound was prepared following a one-pot procedure.

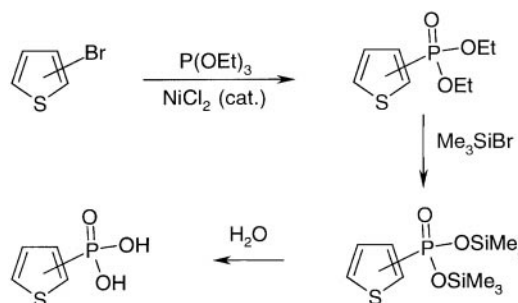
All manipulations were performed under an argon atmosphere using standard Schlenk techniques. THF was distilled

from sodium benzophenone under argon prior to use. Amines were distilled from calcium hydride under argon and kept under an inert atmosphere. Phosphonic acids were dried under vacuum (0.1 mm Hg) at the temperature of their melting point for 2 h. A 2.0 M dimethylzinc solution in toluene was purchased from Aldrich and used directly. $\text{Zn(O}_3\text{PC}_6\text{H}_5) \cdot \text{Bu}^n\text{NH}_2$ was prepared according to ref. 9. Liquid state ^1H and ^{31}P NMR spectra were recorded at room temperature on a Bruker Advance DPX 200 spectrometer operating at 200.13 and 80.96 MHz, respectively. Solid state ^{31}P CP MAS NMR spectra were recorded at room temperature on a Bruker AM 300 spectrometer operating at 121.48 MHz. Powder X-ray diffraction (XRD) patterns were recorded using $\text{Cu-K}\alpha$ radiation. TG analyses were performed with a Netzsch STA 409 thermobalance; temperature range: 20–1000 °C; heating rate: 10 °C min^{-1} ; atmosphere: air; flow: 60 ml min^{-1} . TGA expected relative loss calculations were based on the transformations given in parentheses. IR spectra were taken on a Perkin Elmer 1600 FT by using Nujol mulls.

2.2 Synthesis of thienyl-based phosphonic acids

Thienyl-based phosphonic acids were synthesized following the procedure depicted in Scheme 1.

2.2.1 2-Thienylphosphonic acid. *Diethyl (2-thienyl)phosphonate.* This compound was synthesized according to a modification of the procedure described in ref. 10: to a suspension of anhydrous NiCl_2 (1.19 g, 9.2 mmol) in 2-bromothiophene (18 ml, 184 mmol) at 145 °C was added dropwise 37 ml (220 mmol) of triethylphosphite. During the course of the addition, the reaction mixture turned deep red and bromoethane distilled off readily. After the addition, the reaction mixture was left under stirring for an additional 30 min, filtered and distilled under reduced pressure to afford a colorless oil



Scheme 1 General synthetic route to thienyl-based phosphonic acids.

[38 g, 94%, bp 150–151 °C/3 Torr (lit. 103–104 °C/0.1 Torr¹⁰)]. ¹H NMR (CDCl₃): δ 1.25 (t, 6 H, CH₃), 3.93–4.16 (m, 4 H, OCH₂), 7.07–7.12 (m, 1 H, 5-Th-H), 7.55–7.65 (m, 2 H, 3- and 4-Th-H). ³¹P NMR (CDCl₃): δ 12.17. Anal. Calc. for C₈H₁₃O₃PS (*M*=220): C, 43.60; H, 5.90; O, 21.80; P, 14.00; S, 14.60. Found: C, 43.90; H, 6.06; O, 21.90; P, 13.80; S, 14.34%.

Bistrimethylsilyl (2-thienyl)phosphonate. The bistrimethylsilyl ester was prepared according to the method described in ref. 11 from 10.0 g (45.4 mmol) of diethyl (2-thienyl)phosphonate in 10 ml of CH₂Cl₂ and 18.1 g (118.3 mmol) of Me₃SiBr. Fractional distillation of the resulting blue mixture yielded a colorless liquid (9.7 g, 69%, bp 74 °C/0.01 Torr). ¹H NMR (CDCl₃): δ 0.19 [s, 18 H, Si(CH₃)₃], 7.03–7.04 (m, 1 H, 5-Th-H), 7.53–7.46 (m, 2 H, 3- and 4-Th-H).

2-Thienylphosphonic acid. 3.1 g of bistrimethylsilyl (2-thienyl)phosphonate were poured into a large excess of water under vigorous stirring. After 2 h, the aqueous phase was extracted with CH₂Cl₂ (3 × 10 ml) and evaporated under vacuum to yield the acid as a white solid (1.66 g, 100%, mp 124–126 °C). ¹H NMR (CD₃COCD₃): δ 7.09–7.13 (m, 1 H, 5-Th-H), 7.50–7.53 (m, 1 H, 3-Th-H), 7.75–7.78 (m, 1 H, 4-Th-H), 8.96 (br s, 2 H, OH). ³¹P NMR (CD₃COCD₃): δ 12.85. Anal. Calc. for C₄H₅O₃PS (*M*=164): C, 29.27; H, 3.07; O, 29.25; P, 18.87; S, 19.50. Found: C, 28.83; H, 2.84; O, 28.98; P, 20.60; S, 18.75%.

2.2.2 3-Thienylphosphonic acid. Diethyl (3-thienyl)phosphonate. The same procedure was used as for diethyl (2-thienyl)phosphonate: colorless oil (30 g, 60%, bp 89–92 °C/0.008 Torr). ¹H NMR (CDCl₃): δ 1.34 (t, 6 H, CH₃), 4.08–4.18 (m, 4 H, OCH₂), 7.30–7.47 (m, 2 H, 2- and 5-Th-H), 7.98–8.04 (m, 1 H, 4-Th-H). ³¹P NMR (CDCl₃): δ 13.56. Anal. Calc. for C₈H₁₃O₃PS (*M*=220): C, 43.60; H, 5.90; O, 21.80; P, 14.00; S, 14.60. Found: C, 44.00; H, 5.96; O, 22.55; P, 12.75; S, 14.45%.

3-Thienylphosphonic acid. As above for 2-thienylphosphonic acid, the intermediate bistrimethylsilyl ester was not isolated: white solid (97%, mp 130–131 °C). ¹H NMR (CD₃COCD₃): δ 7.13 (br s, 2 H, OH), 7.30–7.35 (m, 1 H, 5-Th-H), 7.55–7.60 (m, 1 H, 4-Th-H), 7.96–8.02 (m, 1 H, 2-Th-H). ³¹P NMR (CD₃COCD₃): δ 10.68. Anal. Calc. for C₄H₅O₃PS (*M*=164): C, 29.27; H, 3.07; O, 29.25; P, 18.87; S, 19.50. Found: C, 28.29; H, 2.97; O, 29.05; P, 21.18; S, 18.75%.

2.2.3 Thiophen-3-ylmethylphosphonic acid. The thiophen-3-ylmethylphosphonic acid diethyl ester was synthesized according to ref. 12.

Thiophen-3-ylmethylphosphonic acid. Same procedure as for 3-thienylphosphonic acid: white solid (81%, mp 167–169 °C). ¹H NMR (CD₃COCD₃): δ 3.17 (s, 2 H, CH₂-Th), 7.09–7.13 (m, 1 H, 4-Th-H), 7.38–7.42 (m, 2 H, 2- and 5-Th-H). ³¹P NMR (CD₃COCD₃): δ 27.7. Anal. Calc. for C₅H₇O₃PS (*M*=178): C, 33.71; H, 3.93; O, 26.97; P, 17.41; S, 17.98. Found: C, 33.29; H, 4.01; O, 26.23; P, 17.05; S, 17.75%.

2.3 Synthesis of zinc phosphonates

XRD, TGA and ³¹P CP MAS NMR results are given in Tables 1 and 2.

2.3.1 Zn(O₃PC₆H₅) gel formation. Zn(O₃PC₆H₅) 1a. In a typical experiment, a ZnMe₂ toluene solution (4.9 ml, 9.7 mmol) was diluted to a volume of 15 ml with THF and cooled to ca. –40 °C. An equimolar amount of a solution of phenylphosphonic acid (1.56 g, 9.7 mmol) in THF (9 ml) was added dropwise over 1 min. Methane evolution was immediately noticed while a translucent gel slowly developed. The reaction mixture was then allowed to return to room temperature and showed a milky appearance. After stirring

for 3 h at room temperature, the solid was filtered off under argon, washed with dry THF and dried under vacuum at 80 °C to afford **1a** as a white powder (1.83 g, 85%). Anal. Calc. for C₆H₅O₃PZn (*M*=221.4): C, 32.54; H, 2.28; O, 21.68; P, 13.98; Zn, 29.52. Found: C, 33.08; H, 2.39; P, 13.95; Zn, 26.80%.

Using the same experimental conditions as for **1a**: Zn(O₃PCH₃). White powder (89%). Anal. Calc. for CH₃O₃PZn (*M*=159.4): C, 7.55; H, 1.89; O, 31.19; P, 19.49; Zn, 40.88. Found: C, 8.28; H, 2.23; P, 19.48; Zn, 36.84%. Zn[O₃P(2-C₄H₃S)]. White powder (87%). Anal. Calc. for C₄H₃O₃PSZn (*M*=227.4): C, 21.16; H, 1.33; O, 21.14; P, 13.64; S, 14.12; Zn, 28.79. Found: C, 20.75; H, 1.50; P, 12.62; S, 13.04; Zn, 26.63%. Zn[O₃P(3-C₄H₃S)]. White powder (94%). Anal. Calc. for C₄H₃O₃PSZn (*M*=227.4): C, 21.16; H, 1.33; O, 21.14; P, 13.64; S, 14.12; Zn, 28.79. Found: C, 21.86; H, 1.66; P, 14.25; S, 13.28; Zn, 25.00%. Zn[O₃PCH₂(3-C₄H₃S)]. White powder (74%). Anal. Calc. for C₅H₅O₃PSZn (*M*=241.5): C, 24.87; H, 2.09; O, 19.88; P, 12.82; S, 13.27; Zn, 27.07. Found: C, 25.00; H, 2.47; P, 12.24; S, 12.45; Zn, 23.64%.

2.3.2 Hydration of zinc phosphonates. Zn(O₃PC₆H₅)·H₂O 2a. 1a (0.55 g, 2.5 mmol) was suspended in 5 ml of deionized water for 15 h at room temperature. The resulting white solid was washed with ethanol, filtered and dried at room temperature (0.56 g, 93%). Anal. Calc. for C₆H₇O₄PZn (*M*=239.5): C, 30.09; H, 2.95; O, 26.73; P, 12.93; Zn, 27.29. Found: C, 30.20; H, 3.03; P, 12.27; Zn, 24.67%.

Using the same experimental conditions as for **2a**: Zn(O₃PCH₃)·H₂O. White powder (73%). Anal. Calc. for CH₃O₄PZn (*M*=177.4): C, 6.77; H, 2.82; O, 36.08; P, 17.46; Zn, 36.85. Found: C, 6.92; H, 2.74; P, 17.28; Zn, 35.60%. Zn[O₃P(2-C₄H₃S)]·H₂O. White powder (76%). Anal. Calc. for C₄H₅O₄PSZn (*M*=245.5): C, 19.57; H, 2.05; O, 26.07; P, 12.62; S, 13.04; Zn, 26.63. Found: C, 18.90; H, 1.92; P, 12.52; S, 12.40; Zn, 23.61%. Zn[O₃P(3-C₄H₃S)]·H₂O. White powder (79%). Anal. Calc. for C₄H₅O₄PSZn (*M*=245.5): C, 19.57; H, 2.05; O, 26.07; P, 12.62; S, 13.04; Zn, 26.63. Found: C, 22.15; H, 1.86; P, 13.66; S, 14.10; Zn, 22.76%. Zn[O₃PCH₂(3-C₄H₃S)]·H₂O. White powder (89%). Anal. Calc. for C₅H₇O₄PSZn (*M*=259.5): C, 23.14; H, 2.72; O, 24.66; P, 11.93; S, 12.35; Zn, 25.19. Found: C, 23.96; H, 2.33; P, 11.81; S, 12.48; Zn, 24.73%.

2.4 Intercalation of amines

2.4.1 Into the gel-like zinc phenylphosphonate. Zn(O₃PC₆H₅)·BuⁿNH₂ 3a. The same procedure was used as for **1a** except that after the evolution of methane, a THF (10 ml) solution of *n*-butylamine (0.71 g, 9.7 mmol) was added to the gel suspension. After filtration and drying, a white solid was obtained (0.20 g, 70%). Anal. Calc. for C₁₀H₁₆NO₃PZn (*M*=294.6): C, 40.77; H, 5.47; N, 4.76; O, 16.29; P, 10.51; Zn, 22.19. Found: C, 39.28; H, 5.38; N, 4.57; P, 9.29; Zn, 23.82%.

2.4.2 Impregnation procedure. Amine intercalation into zinc phosphonates was achieved according to ref. 9.

Zn(O₃PC₆H₅)·2Hex^cNH₂ **4b.** The intercalate was recovered as a white solid (80%) after 15 d of contact under stirring at room temperature. Anal. Calc. for C₁₈H₂₉N₂O₃PZn (*M*=417.8): C, 51.75; H, 7.00; N, 6.71; O, 11.49; P, 7.41; Zn, 15.65. Found: C, 46.82; H, 6.85; N, 5.86; P, 7.05; Zn, 12.35%.

2.4.3 One-pot procedure. Zn(O₃PC₆H₅)·BuⁿNH₂ 3c. 1.2 ml of a ZnMe₂ solution (2.36 mmol) in toluene was diluted to 10 ml with THF and cooled at ca. –40 °C. *n*-Butylamine (0.17 g, 2.30 mmol) was then added and the mixture stirred at this temperature for 10 min; no appreciable modification of the mixture or gas evolution were noted. A solution of phenylphosphonic acid (0.36 g, 2.30 mmol) in THF (10 ml) was then

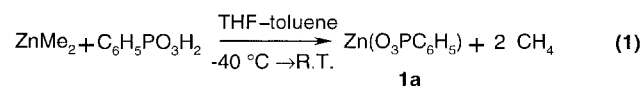
added over 1 min leading to the observations found for **1a**. After filtration and drying, a white solid was obtained (0.63 g, 93%). Anal. Calc. for $C_{10}H_{16}NO_3PZn$ ($M=294.6$): C, 40.77; H, 5.47; N, 4.76; O, 16.29; P, 10.51; Zn, 22.19. Found: C, 41.61; H, 5.76; N, 5.03; P, 10.40; Zn, 20.05%.

Using the same procedure as for **3c**: $Zn(O_3PC_6H_5) \cdot Hex^iNH_2$ **4c**. White solid (95%). Anal. Calc. for $C_{12}H_{18}NO_3PZn$ ($M=320.6$): C, 44.95; H, 5.66; N, 4.37; O, 14.97; P, 9.66; Zn, 20.39. Found: C, 47.02; H, 6.23; N, 4.96; P, 8.98; Zn, 15.80%. $Zn(O_3PC_6H_5) \cdot Pen^iNH_2$. White solid (82%). Anal. Calc. for $C_{11}H_{18}NO_3PZn$ ($M=308.6$): C, 42.81; H, 5.88; N, 4.54; O, 15.55; P, 10.03; Zn, 21.18. Found: C, 42.38; H, 5.77; N, 4.45; P, 10.01; Zn, 20.33. $Zn(O_3PCH_3) \cdot Bu^iNH_2$. White powder (98%). Anal. Calc. for $C_5H_{14}NO_3PZn$ ($M=232.5$): C, 25.83; H, 6.07; N, 6.02; O, 20.64; P, 13.32; Zn, 28.11. Found: C, 23.37; H, 5.78; N, 5.15; P, 13.68; Zn, 26.73%. $Zn[O_3P(2-C_4H_3S)] \cdot Pen^iNH_2$. White powder (80%). Anal. Calc. for $C_9H_{16}NO_3PSZn$ ($M=314.5$): C, 34.36; H, 5.13; N, 4.45; O, 15.26; P, 9.84; S, 10.19; Zn, 20.78. Found: C, 35.85; H, 5.34; N, 4.67; P, 7.74; S, 8.83; Zn, 18.63%. $Zn[O_3P(3-C_4H_3S)] \cdot Pen^iNH_2$. White powder (91%). Anal. Calc. for $C_9H_{16}NO_3PSZn$ ($M=314.5$): C, 34.36; H, 5.13; N, 4.45; O, 15.26; P, 9.84; S, 10.19; Zn, 20.78. Found: C, 34.18; H, 5.02; N, 3.96; P, 10.60; S, 10.86; Zn, 19.12%. $Zn[O_3PCH_2(3-C_4H_3S)] \cdot Pen^iNH_2$. White powder (91%). Anal. Calc. for $C_{10}H_{18}NO_3PSZn$ ($M=328.7$): C, 36.54; H, 5.52; N, 4.26; O, 14.60; P, 9.42; S, 9.72; Zn, 19.89. Found: C, 34.91; H, 5.78; N, 4.06; P, 8.72; S, 8.87; Zn, 18.23%.

3 Results and discussion

3.1 Zinc phosphonates by the organometallic route [eqn. (1)]

Typically, an equimolar amount of phenylphosphonic acid (THF solution) was added to dimethylzinc (2.0 M solution in toluene) at $-40^\circ C$. Methane evolution was immediately noticed and the clear solution was allowed to warm. Under slow stirring, a translucent gel slowly developed which finally collapsed into a milky suspension within a few minutes at ambient temperature. Stirring was maintained for 2 h to yield **1a** (see the general remarks in Section 2 for the notation of the compounds) as a white xerogel after filtration and drying under vacuum.



Spectroscopic data (Table 1) and the elemental analyses are in accord with the expected formula and are essentially unchanged compared to those of the dehydrated zinc phenylphosphonate **1b** prepared by heating the monohydrate *in vacuo* at $400^\circ C$.¹⁴ The powder X-ray diffraction (XRD) pattern is characteristic of a layered structure and displays an interlayer distance of 14.4 Å (Fig. 1). The broadened peak widths may be attributed either to severe distortions in the layered structure or

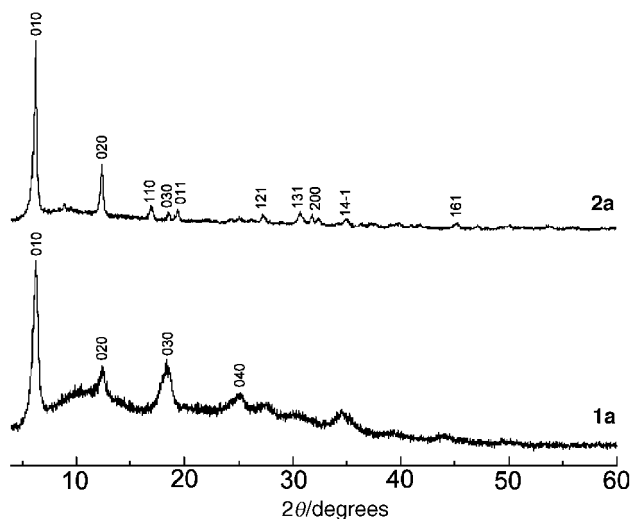


Fig. 1 Powder XRD pattern of $Zn(O_3PC_6H_5)$ **1a** and $Zn(O_3PC_6H_5) \cdot H_2O$ **2a**.

to an incipient stage of crystallization which is consistent with the gel-like structure of the solid. The ^{31}P CP MAS NMR of **1a** shows a single peak at δ 20.0 which is consistent with a unique chemical environment for the phosphorus atoms. The signal appears to be displaced by 3.3 ppm from the position observed for $Zn(O_3PC_6H_5) \cdot H_2O$ (δ 23.3) and indicates a decrease in the coordination number of the zinc atoms.¹³

Fig. 2 shows the thermogravimetric curve obtained during the thermolysis of **1a** up to $1000^\circ C$ in an air flow. No weight loss was observed up to $500^\circ C$. At higher temperature, the removal of the phenyl groups takes place. The total weight loss of 31.8% is close to the expected value of 31.2% for the reaction $1a \rightarrow \frac{1}{2} Zn_2P_2O_7$ (as identified by XRD). Furthermore, **1a** quickly absorbs moisture from the air to form the mono-

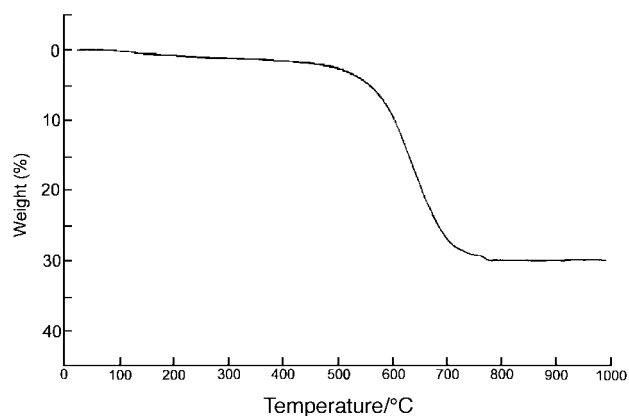


Fig. 2 Thermogravimetric curve obtained during the thermolysis of **1a** up to $1000^\circ C$ in an air flow.

Table 1 Interlayer distances, TG and NMR results of zinc phosphonates^a

Compound	<i>d</i> spacing/Å	$\Delta m/m$ (%)	^{31}P CP MAS NMR (δ)
$Zn(O_3PC_6H_5)$	14.4 (14.30) ¹⁴	31.8 (31.2)	20.0
$Zn(O_3PC_6H_5) \cdot H_2O$	14.38 (14.34) ¹⁴	35.1 (36.4)	23.3
$Zn(O_3PCH_3)$	6.9 (6.94) ¹⁵	5.5 (4.4)	32.8 (32.6) ¹³
$Zn(O_3PCH_3) \cdot H_2O$	8.72 (8.73) ¹⁵	14.3 (14.1)	34.7
$Zn[O_3P(2-C_4H_3S)]$	13.4	32.1 (33.0)	14.1
$Zn[O_3P(2-C_4H_3S)] \cdot H_2O$	13.6	38.0 (37.9)	17.4
$Zn[O_3P(3-C_4H_3S)]$	14.2	34.4 (33.0)	14.9
$Zn[O_3P(3-C_4H_3S)] \cdot H_2O$	14.3	37.4 (37.9)	18.7
$Zn[O_3PCH_2(3-C_4H_3S)]$	14.9	38.8 (36.9)	29.4
$Zn[O_3PCH_2(3-C_4H_3S)] \cdot H_2O$	14.6	40.1 (41.3)	31.4

^aTheoretical or literature values are in parentheses.

hydrate $\text{Zn}(\text{O}_3\text{PC}_6\text{H}_5)\cdot\text{H}_2\text{O}$ **2a**.¹⁴ Hydration of **1a** led to **2a** with a noticeable improvement of the crystallinity as shown by XRD. A comparison between the XRD patterns (Fig. 1) and the chemical analyses of both **2a** and a reference compound **2b** prepared according to the literature¹⁴ shows that they are almost identical.

The above method has been extended to a series of phosphonic acids (Table 1) and the corresponding layered anhydrous derivatives have been obtained in high yields. As reported previously for zinc phenylphosphonate,¹⁴ both anhydrous and monohydrated zinc phosphonates (with the exception of zinc methylphosphonate¹⁵) retain almost the same interlayer distance. Moreover, as observed for **1a** and **2a**, ³¹P chemical shifts systematically move downfield when passing from the anhydrous to the monohydrate phosphonate. Interestingly, zinc 2-thienylphosphonate displays a shorter interlayer distance than its 3-isomer. Taking into account that both isomers have a similar steric bulk, this difference may arise from interactions between sulfur atoms in the organic layers allowing a slight interpenetration of the organic subnetworks. For zinc thiophen-3-ylmethylphosphonate the short interlayer distance (14.9 Å) with respect to zinc 2- or 3-thienylphosphonates indicates that the thienyl rings lie in a pseudo-face-to-face configuration in the interlayer space (Fig. 3).

3.2 Intercalation of amines *via* the organometallic routes

When contacted with neat liquid primary amines, the layered anhydrous zinc phosphonate $\text{Zn}(\text{O}_3\text{P}_6\text{H}_5)$ and its monohydrate $\text{Zn}(\text{O}_3\text{PC}_6\text{H}_5)\cdot\text{H}_2\text{O}$ are known to intercalate one equivalent of amine to form compounds of composition $\text{Zn}(\text{O}_3\text{PC}_6\text{H}_5)\cdot\text{RNH}_2$. The amine molecules are regularly bonded to vacant coordination sites at the zinc atoms of the host and the layered structure is preserved. This process requires long contact times [72 h for $\text{Zn}(\text{O}_3\text{PC}_6\text{H}_5)$ and 240 h for $\text{Zn}(\text{O}_3\text{PC}_6\text{H}_5)\cdot\text{H}_2\text{O}$], a large excess of amine, and is restricted to primary amines. This behavior is presumably due to steric constraints and to the slow diffusion rate of the amine molecules into the host layered material.⁹

In sharp contrast, the organometallic route offers some advantages: first, the gel-like nature of **1a** would allow a better diffusion of the amine into the host material leading to a reduction of the contact time. Second, the introduction of the amine as a template molecule in the early stage of the reaction

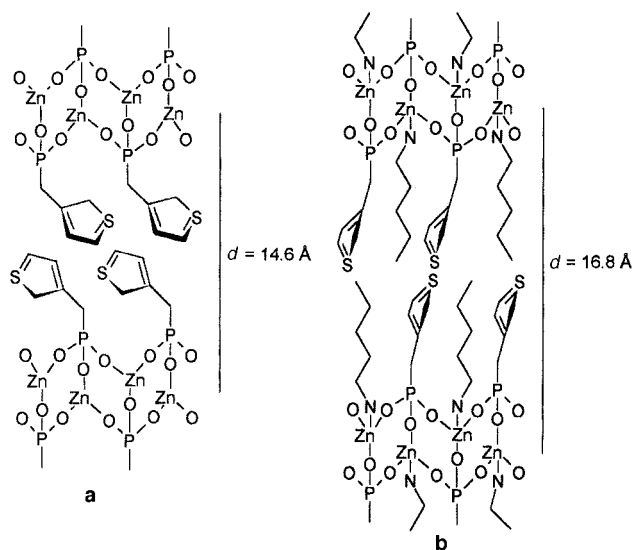


Fig. 3 Schematic representations of zinc thiophen-3-ylmethylphosphonates: (a) pseudo-face-to-face orientation of the hydrated phase and (b) pseudo-edge-to-edge orientation of the amine intercalate.

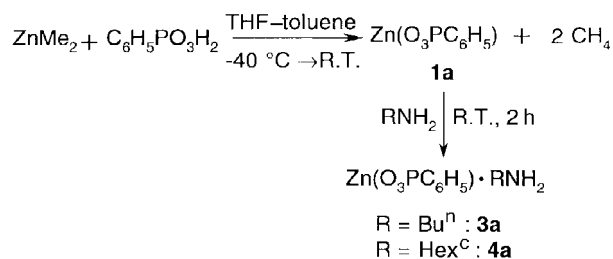
would allow the control of both the structure¹⁶ and the amine content of the final material.

3.2.1 Route A. In a first experiment, we have checked the ability of gel **1a** to intercalate *n*-alkylamines (Scheme 2). Thus, the addition of an equimolar amount of *n*-butylamine to the gel resulting from the reaction of phenylphosphonic acid and ZnMe_2 led to a very fine white precipitate after ambient temperature had been reached. After an additional time of 2 h under stirring, **3a** was obtained as a very fine white powder in high yield.

Both elemental analysis and TGA of **3a** (Fig. 4) clearly show that the amine is quantitatively intercalated (observed weight loss: 25.7%, expected: 24.8%). Moreover, the amine removal, which is characterized by an onset temperature of 195 °C and a clean one-step process, is consistent with an effective regular coordination of the amine molecules at the zinc atoms.⁹ The second weight loss which is observed in the TG curve at *ca.* 500 °C is assigned to the removal of the phenyl groups. The XRD pattern (Fig. 5) of **3a** displays a high crystallinity and the interlayer spacing of 14.4 Å is consistent with the value reported previously.⁹

3.2.2 Route B. In a second experiment, we have investigated the consequences of the presence of the amine during the early stages of the reaction (Scheme 3). The addition of an equimolar amount of phenylphosphonic acid in THF to a $\text{ZnMe}_2\cdot\text{Bu}^n\text{NH}_2$ ¹⁷ solution at -40 °C led to the initial formation of a translucent gel which finally turned into a white precipitate. The solid **3c**, which was recovered after 2 h of stirring, shares the characteristics displayed by **3a**. However, as illustrated by XRD (Fig. 5), differences in crystallinity between **3a** and **3c** are illustrative of a template effect owing to the presence of the amine during the formation of the material.

Intercalation of amines has been extended to the other zinc



Scheme 2 Amine intercalation *via* organometallic route A.

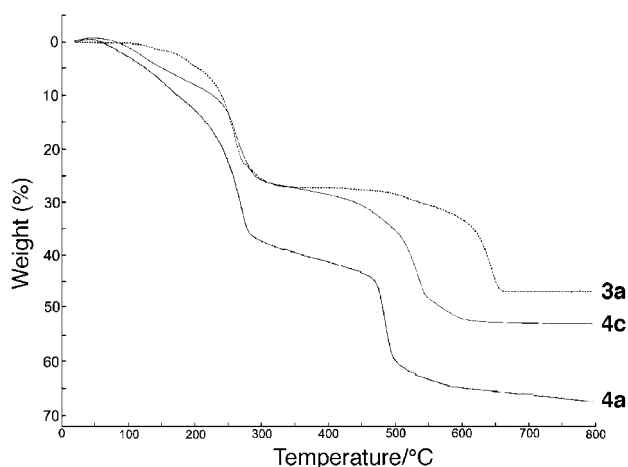


Fig. 4 Thermogravimetric curve obtained during the thermolysis of **3a** (dashed line), **4a** and **4c** up to 800 °C in an air flow.

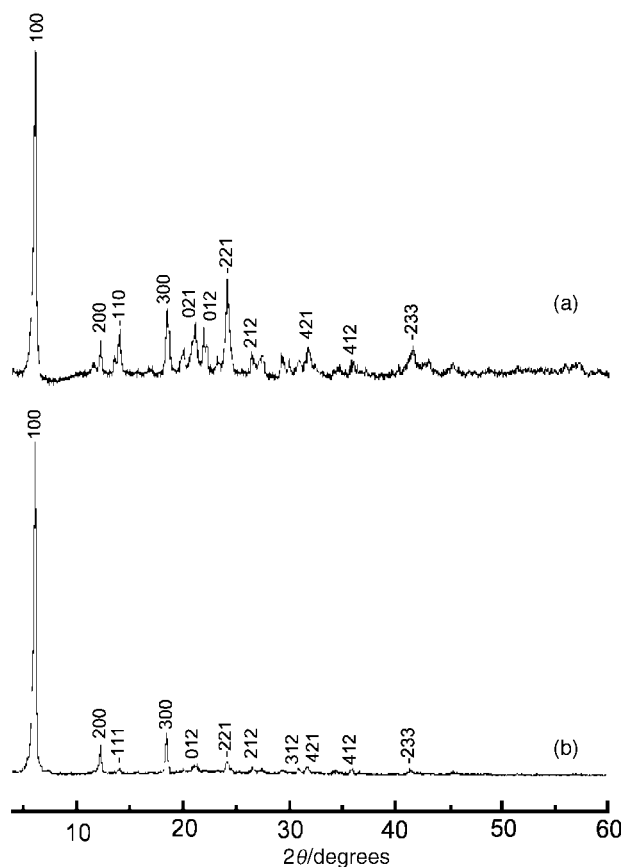
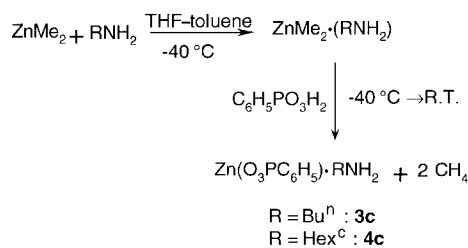


Fig. 5 Powder XRD pattern of $\text{Zn}(\text{O}_3\text{PC}_6\text{H}_5)\cdot\text{Bu}^n\text{NH}_2$ (a) route A (**3a**) and (b) route B (**3c**).



Scheme 3 Amine intercalation via organometallic route B.

phosphonates and results are shown in Table 2. As measured by TG, amine intercalation occurs to a high extent for each phosphonate. In every case, the upfield displacement of the ^{31}P chemical shift is consistent with a decrease in the phosphonate connectivity leading to the expected tetra-coordination of the zinc atoms in the layers.^{9,13}

As shown by XRD, the increase of the interlayer distances depends on the number of carbon atoms in the *n*-alkylamine chains; *n*-pentylamine intercalates led generally to values of *ca.* 15.5 Å.⁹ The value observed with the thiophen-3-ylmethyl-

phosphonate derivative (16.8 Å) reflects the steric bulk arising from the coordination of the *n*-pentylamine at the zinc atoms. These constraints prevent pseudo-face-to-face orientation of the thienyl rings (Fig. 3). Rather a pseudo-edge-to-edge orientation is consistent with the observed interlayer distance of 16.8 Å.

For a more crowded amine such as cyclohexylamine, the TGA curve (Fig. 4) shows that intercalation is almost quantitative using this procedure (amine weight loss: observed: 29%, expected: 31%). The overall weight loss of 53.1% at 800 °C is close to the expected value for the transformation $\mathbf{4c} \rightarrow \frac{1}{2} \text{Zn}_2\text{P}_2\text{O}_7$ (-55%). The presence of four sharp bands at 3298, 3249, 3161 (NH_2 stretching) and 1593 cm^{-1} (NH_2 bending) in the IR spectrum (Fig. 6) indicates effective regular coordination of cyclohexylamine to zinc.⁹ On the other hand, when compared to the other zinc phenylphosphonate *n*-alkylamine intercalates (Table 2), the decrease of the amine volatilization temperature (onset temperature: *ca.* 80 °C) indicates that the strength of coordination at the zinc atoms is significantly lower for cyclohexylamine.

The XRD pattern of **4c** shows a poorly crystallized layered structure with an interlayer spacing of 14.3 Å (Fig. 7). The unique peak observed in the ^{31}P CP MAS NMR spectrum at δ 12.4 (Fig. 7) is indicative of both chemical and structural homogeneity in the material. However, the difference between the chemical shift observed here and that for the Bu^nNH_2 intercalate **3c** (δ 18.7) reflects a dramatic environmental change around the phosphorus atoms. This difference is also illustrated by comparison of the IR spectra of **3c** and **4c** (Fig. 6): examination of the PO_3M stretching pattern (1200–950 cm^{-1}) which is very sensitive to coordination changes around the metal centers, indicates that the inorganic layers of **4c** display a quite different structure than the general structure observed with *n*-alkylamines.⁹ These results indicate that the role of the amine is as a template in the formation of the solid.

In order to make a comparison with the organometallic routes, attempted intercalation by contact of the anhydrous zinc phenylphosphonate **1b** with an excess of cyclohexylamine was performed. Surprisingly, after 15 days, chemical analysis of

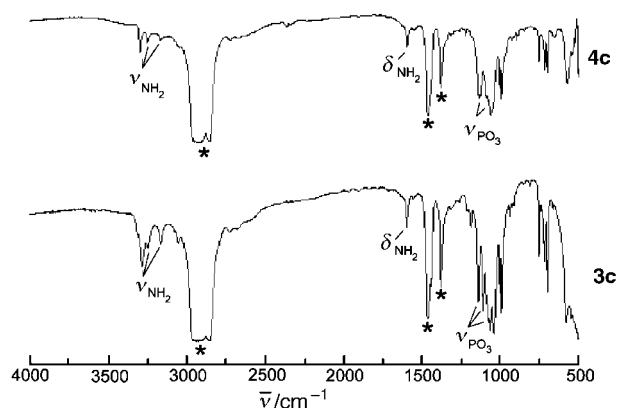


Fig. 6 FTIR spectra (Nujol mulls) of the Bu^nNH_2 intercalate **3c** and the Hex^cNH_2 intercalate **4c**. Nujol bands are denoted by an asterisk.

Table 2 Interlayer distances, TG and NMR results of *n*-alkylamine intercalates^a

Compound	<i>d</i> spacing/Å	$\Delta m/m$ (%)	Onset temperature/°C	^{31}P CP MAS NMR (δ)
$\text{Zn}(\text{O}_3\text{PC}_6\text{H}_5)\cdot\text{Bu}^n\text{NH}_2$	14.4 (14.4) ⁹	25.7 (24.8)	140	18.8
$\text{Zn}(\text{O}_3\text{PC}_6\text{H}_5)\cdot\text{Pen}^n\text{NH}_2$	15.8 (15.8) ⁹	26.6 (28.2)	130	19.3
$\text{Zn}(\text{O}_3\text{PCH}_3)\cdot\text{Bu}^n\text{NH}_2$	13.6 (13.6) ¹⁵	29.3 (31.4)	160	22.9 (27.7) ¹³
$\text{Zn}[\text{O}_3\text{P}(2\text{-C}_4\text{H}_3\text{S})]\cdot\text{Pen}^n\text{NH}_2$	15.5	27.0 (28.9)	118	12.4
$\text{Zn}[\text{O}_3\text{P}(3\text{-C}_4\text{H}_3\text{S})]\cdot\text{Pen}^n\text{NH}_2$	15.3	27.8 (28.9)	107	13.9
$\text{Zn}[\text{O}_3\text{PCH}_2(3\text{-C}_4\text{H}_3\text{S})]\cdot\text{Pen}^n\text{NH}_2$	16.8	25.4 (26.5)	98	24.1

^aTheoretical or literature values are in parentheses. TG results are related to loss of amine.

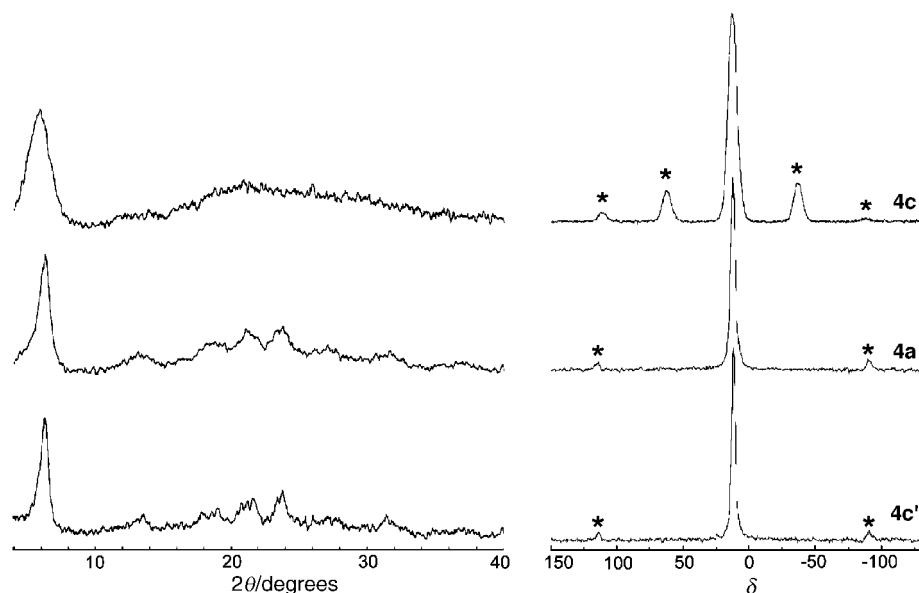


Fig. 7 XRD patterns and ^{31}P CP MAS NMR spectra of the cyclohexylamine intercalate **4a** (1:2), **4c** (1:1) and **4c'** (1:2). Spinning side bands are denoted by an asterisk.

the solid **4b** indicated that nearly two equivalents of amine rather than one are intercalated.¹⁸ Moreover, the XRD pattern of the solid reveals an extensive destruction of the initial host structure. Knowing that, even in the presence of an excess of primary linear *n*-alkylamine and whatever the procedure adopted, only 1:1 intercalates are formed,¹⁹ these results have prompted us to investigate the action of an excess of cyclohexylamine following routes A (**4a**) and B (**4c'**).

Whatever the procedure, analogous characteristics are observed for **4a** and **4c'**: TG curves show that two amine molecules are intercalated giving the empirical formula $\text{Zn}(\text{O}_3\text{PC}_6\text{H}_5) \cdot 2\text{Hex}^c\text{NH}_2$ (amine weight loss observed: 42.2%, expected: 45%), XRD patterns (Fig. 7) show layered structures ($d = 14.3 \text{ \AA}$) with an increase in the crystallinity when compared to **4c**. Interestingly, as observed for the 1:1 cyclohexylamine intercalate, a unique peak is seen in the ^{31}P CP MAS NMR spectra at $\delta \text{ ca. } 13$. As observed by XRD, the improvement in crystallinity brought by the second amine molecule is reflected by a narrowing of the NMR peaks from **4c**

to **4c'**. The IR spectrum displays $\text{R}-\text{NH}_2 \rightarrow \text{Zn}$ stretching bands characteristic of a homogeneous structure in which all the amine molecules are coordinated to zinc atoms.

Considering that the ^{31}P chemical shifts move upfield as the connectivity decreases (Table 3),¹³ it is reasonable to postulate that the phenylphosphonate moieties adopt a (011) connectivity leading to a ZnN_2O_2 tetrahedral arrangement for the 1:2 cyclohexylamine intercalates. Cyclohexylamine intercalates may thus be related to the polymeric zinc phosphate-diamine adduct $\{\text{Zn}[\text{O}_2\text{P}(\text{OBu}^t)_2][\text{H}_2\text{N}(\text{CH}_2)_6\text{NH}_2]\}_n$ described by Tilley and coworkers⁷ (Fig. 8). The bulkiness of the cyclohexyl groups prevents the formation of the 2D network observed with the other linear *n*-alkylamines, but rather leads to the formation of 1D polymeric chains in which a (011) phosphonate connectivity is encountered. As indicated by NMR spectroscopy, this situation would be established in the 1:1 intercalate for which the zinc atoms display a coordination vacancy which is readily filled when the solid is contacted with additional amine.

Table 3 Relationship between ^{31}P chemical shifts and phosphonate connectivity¹³

Compound	^{31}P CP MAS NMR δ	Connectivity	Zn environment
$\text{Zn}(\text{O}_3\text{PC}_6\text{H}_5) \cdot \text{H}_2\text{O}$	23.3	(122)	
$\text{Zn}(\text{O}_3\text{PC}_6\text{H}_5)$	20.0	(112)	
$\text{Zn}(\text{O}_3\text{PC}_6\text{H}_5) \cdot \text{Bu}^t\text{NH}_2$	18.8	(111)	
$\text{Zn}(\text{O}_3\text{PC}_6\text{H}_5) \cdot \text{Hex}^c\text{NH}_2$	12.4	(011)	
$\text{Zn}(\text{O}_3\text{PC}_6\text{H}_5) \cdot 2\text{Hex}^c\text{NH}_2$	13.0	(011)	

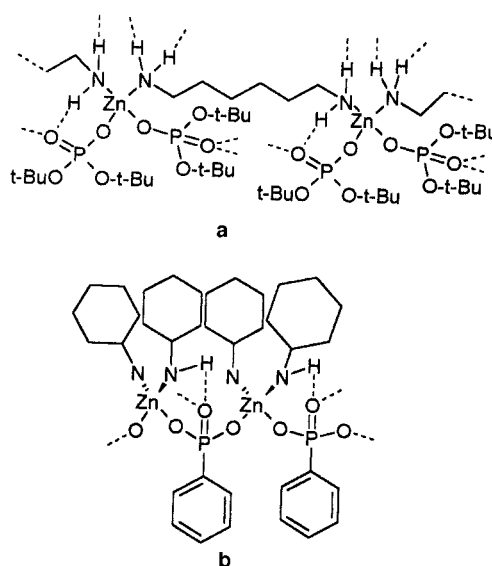


Fig. 8 Schematic drawings of (a) polymeric $\{\text{Zn}[\text{O}_2\text{P}(\text{OBu}^t)_2][\text{H}_2\text{N}(\text{CH}_2)_6\text{NH}_2]\}_n$ ⁷ and (b) $\text{Zn}(\text{O}_3\text{PC}_6\text{H}_5) \cdot 2\text{Hex}^c\text{NH}_2$.

4 Conclusion

In conclusion, zinc phosphonates and their intercalates have been successfully prepared by a non-hydrolytic organometallic route. The presence of the amine in the early stage of the formation of the zinc phosphonates affords improvements both in the variety of intercalated amines and in ease of intercalation: first, contact times are considerably shortened and second, the amines can be used in stoichiometric amounts. Moreover, the intercalation of crowded amines such as cyclohexylamine has underlined two additional interesting features: the control of the intercalation stoichiometry into the layered host and access to new homogeneous structures directed by the template effect of the amine.

References

- 1 L. Ouahab, *Chem. Mater.*, 1997, **9**, 1909; P. Judenstein and C. Sanchez, *J. Mater. Chem.*, 1996, **6**, 511; U. Schubert, N. Hüsing and A. Lorenz, *Chem. Mater.*, 1995, **7**, 2010.
- 2 A. Clearfield, *Prog. Inorg. Chem.*, 1998, 371; D. O'Hare, in *Inorganic Materials*, ed. D. W. Bruce and D. O'Hare, J. Wiley & Sons, New York, 2nd edn., 1997, p. 172; G. Alberti, M. Casciola, U. Costantino and R. Vivani, *Adv. Mater.*, 1996, **8**, 291.
- 3 K. J. Scott, Y. Zhang, R.-C. Wang and A. Clearfield, *Chem. Mater.*, 1995, **7**, 1095.
- 4 G. B. Hix and K. D. M. Harris, *J. Mater. Chem.*, 1998, **8**, 579.
- 5 R. J. P. Corriu, D. Leclercq, P. H. Mutin, L. Sarlin and A. Vioux, *J. Mater. Chem.*, 1998, **8**, 1827.
- 6 M. G. Walawalkar, R. Murugavel, A. Voigt, H. W. Roesky and H.-G. Schmidt, *J. Am. Chem. Soc.*, 1997, **119**, 4656; Y. Yang, H.-G. Schmidt, M. Noltemeyer, J. Pinkas and H. W. Roesky, *J. Chem. Soc., Dalton Trans.*, 1996, 3609.
- 7 C. G. Lugmair, T. D. Tilley and A. L. Rheingold, *Chem. Mater.*, 1997, **9**, 339; Y. Yang, J. Pinkas, M. Noltemeyer, H.-G. Schmidt and H. W. Roesky, *Angew. Chem., Int. Ed.*, 1999, **38**, 664.
- 8 A. Voigt, R. Murugavel, E. Parisini and H. W. Roesky, *Angew. Chem., Int. Ed. Engl.*, 1996, **35**, 748; A. Keys, S. Bott and A. Barron, *J. Chem. Soc., Chem. Commun.*, 1995, 2339; M. L. Montero, A. Voigt, M. Teichert, I. Usón and H. W. Roesky, *Angew. Chem., Int. Ed. Engl.*, 1995, **34**, 2504; F. E. Hahn, B. Schneider and F. W. Reier, *Z. Naturforsch. Teil B*, 1990, **45**, 134.
- 9 Y. P. Zhang, K. J. Scott and A. Clearfield, *J. Mater. Chem.*, 1995, **5**, 315; D. M. Poojary and A. Clearfield, *J. Am. Chem. Soc.*, 1995, **117**, 11278.
- 10 P. Tavs, *Chem. Ber.*, 1970, **103**, 2428.
- 11 C. E. McKenna, M. T. Higa, N. H. Cheung and M. C. McKenna, *Tetrahedron Lett.*, 1977, 155.
- 12 M. Iwao, M. L. Lee and R. N. Castle, *Heterocycl. Chem.*, 1980, **17**, 1259.
- 13 S. Drumel, P. Janvier, M. Bujoli-Doeuff and B. Bujoli, *J. Mater. Chem.*, 1996, **6**, 1843; D. Massiot, S. Drumel, P. Janvier, M. Bujoli-Doeuff and B. Bujoli, *Chem. Mater.*, 1997, **9**, 6.
- 14 K. J. Frink, R.-C. Wang, J. L. Colón and A. Clearfield, *Inorg. Chem.*, 1991, **30**, 1438; K. J. Martin, P. J. Squattrito and A. Clearfield, *Inorg. Chim. Acta*, 1989, **155**, 7; G. Cao, H. Lee, M. Lynch and T. E. Mallouk, *Inorg. Chem.*, 1988, **27**, 2781; D. Cunningham, P. J. D. Hennelly and T. Deeney, *Inorg. Chim. Acta*, 1979, **37**, 95.
- 15 G. Cao and T. E. Mallouk, *Inorg. Chem.*, 1991, **30**, 1434.
- 16 For a review see: G. Ferey, *C. R. Acad. Sci. Paris, Sér. IIC*, 1998, **1**, 1.
- 17 The adduct is formed by direct reaction of the amine with $ZnMe_2$, see: A. C. Jones, P. O'Brien and J. R. Walsh, *Inorg. Synth.*, 1997, **31**, 15.
- 18 Several bis-amino complexes of $Zn(II)$ salts including phosphate esters⁷ are known in the literature, but, to our knowledge, only one reference deals with bis-amino complexes of zinc phosphonates: T. Kiss, J. Balla, G. Nagy, H. Kozłowski and J. Kowalik, *Inorg. Chim. Acta*, 1987, **138**, 25.
- 19 Intercalates **4a** and **4c** are obtained in an identical form by using a ten-fold excess of *n*-butylamine.

Paper 9/02854D